Open-spandrel arch analysis assuming continuity of structure

Autor(en): **Beaufoy, L.A.**

Objekttyp: **Article**

Zeitschrift: **IABSE publications = Mémoires AIPC = IVBH Abhandlungen**

Band (Jahr): **13 (1953)**

PDF erstellt am: **22.09.2024**

Persistenter Link: https://doi.org/10.5169/seals-13193

Open-Spandrel Arch Analysis Assuming Continuity of Structure

Etude des Arcs à Tympan ouvert dans l'hypothèse de la continuité de l'ouvrage

Berechnung des Bogens mit durchbrochenem Aufbau bei Annahme monolithischen Zusammenhangs

Dr. L. A. Beaufoy, M. Sc. (Eng.), A.M.I.C.E., M. I. Mech. E., M. I. Struct. E., M. Am. Soc. C. E., Chartered Civil Engineer, London

Introduction

Because of the incomplete nature of our knowledge of the interaction between the deck, the spandrel columns and the arch rib of a bridge which is monolithic, proper consideration is not given to its effect when designing open-spandrel arches. Designs are commonly based on the assumption that loads are applied directly to the arch rib, whose behaviour is assumed to be uninfluenced by the spandrel columns and deck. The many experiments which have been carried out to study the effect of deck participation have not provided a full picture of the nature of this participation, being limited to the determination of influence lines for the fixed-end reactions and the resultant lines of thrust for temperature stresses. Information is lacking as to the manner in which stresses are distributed quantitatively between the arch rib and the deck, and, although it is known that the deck aids the arch rib, it is not known to what extent this assisting role may be harmful to the deck.

The mathematical analysis of open-spandrel arches by the classical methods is so tedious that it has been regarded by some engineers as virtually impossible unless certain approximations are made. One approximation sometimes used is to neglect the shear in the spandrel columns, or, in other words, to assume these columns to be hinged at both ends. Although such an approximation may seem to be reasonable, especially when the columns are comparatively slender, it is, nevertheless, very misleading. The most important role in deck participation is, as will be seen later, that of the shear resistance of the spandrel columns, which is responsible for transferring a comparatively large thrust to the deck. If there were no such shear resistance no thrust could be transmitted. The near-impossibility of the classical methods of analysis has

therefore led to extensive experimental studies, of which those of WILSON[1]) and FINLAY [2]) may be especially cited.

The object of the present paper is to present a reasonably simple and exact method of theoretical analysis for open-spandrel arch systems, requiring the expenditure of less time and effort than the experimental one. By avoiding the formulation of simultaneous equations, all calculations may be performed by slide-rule. This method of analysis is similar to that for Vierendeel trusses described recently by the author[3]).

The difference between the two systems is that open-spandrel arches are externally statically indeterminate as well as being internally so. It therefore becomes necessary to distinguish between the internal panels and the end (or external) panels to which external moments are applied. The present paper develops the necessary extension to the method of analysis of Vierendeel trusses and carries the structural analysis further so that the elastic constants and stiffness factors for the open-spandrel arch as a whole may be determined, thereby making it possible to calculate the influence lines for the fixed-end reactions. Once these are known, the computations for stresses produced anywhere in the system due to any given loading, temperature changes, or displacements at a support follow readily.

The application of the method is illustrated in some detail by reference to an example of a nine-panel open-spandrel arch[4]) which was the subject of experimental analysis, so that an experimental check on some of the theoretical results is available. It will be found that the agreement between the two sets of results is of a high order.

The author is indebted to A. F. S. DIWAN, formerly a research student in civil engineering working under his direction, for assistance with the computational work, and to C. C. BREARLEY, who prepared the illustrations for press.

Notation and Sign Convention

Symbols are defined when they are first used, but are collected here for convenience of reference.

a denotes panel width.

b denotes difference in height between spandrel posts in a panel.

---

[1]) WILSON, "Tests of Reinforced Concrete Arch Bridges", Publications, I.A.B.S.E., vol. 5, 1938.

[2]) FINLAY, "Deck Participation in Concrete Arch Bridges", Civil Engineering (N. Y.), vol. 2, no. 11, 1932.

[3]) BEAUFOY, "Vierendeel Truss Analysis using Equivalent Elastic Systems", Publications, I.A.B.S.E., vol. 11, 1951.

[4]) WILSON and KLUGE, "Laboratory Tests of Three-span Reinforced-concrete Arch Bridges with Decks on Slender Piers", Bulletin No. 270, University of Illinois Engineering Experiment Station, 1934.

C denotes panel coefficient.
d denotes vertical distance between the elastic centre and the deck of an open-spandrel arch.
d as suffix, denotes that the quantity refers to the deck.
e as suffix, denotes that the quantity refers to a virtual equivalent system.
E denotes Young's modulus.
h, H denote horizontal force; height of spandrel post.
I denotes a centroidal moment or product of inertia.
I_x' $= I_x - (I_{xy}^2/I_y)$.
I_y' $= I_y - (I_{xy}^2/I_x)$.
L denotes length of span.
m, M denote moment.
M_x' $= M_x - (M_y I_{xy}/I_y)$.
M_y' $= M_y - (M_x I_{xy}/I_x)$.
O as suffix, denotes that the quantity refers to the elastic centre.
P denotes normal elastic load on analogous column.
Q denotes shearing force.
r as suffix, denotes that the quantity refers to the arch rib.
$\bar{S}$ denotes elastic area.
T denotes thrust in deck.
v, V denote vertical force.
x, y denote horizontal and vertical co-ordinate distances respectively.
$\bar{x}, \bar{y}$ denote horizontal and vertical co-ordinates respectively of the elastic centre.
x, y, xy as suffixes, denote that the quantity is taken about the x-axis, the y-axis, or axes x, y.
ϕ, Δ, λ denote rotational, horizontal and vertical displacements respectively.
ϕ, Δ, λ as suffixes, denote that the quantity is in respect of applied rotational, horizontal or vertical displacement respectively.

Sign Convention. Unless otherwise stated this is as follows: Moments and rotational displacements are taken as positive when clockwise; horizontal and vertical forces, displacements, and co-ordinate distances as positive when measured to the right and upwards respectively.

The Single Closed Panel

Provided they are in equilibrium, and assuming that deformations due to shear and axial thrust may be disregarded, any system of external forces applied to a closed panel through its joints (Fig. 1) may be reduced to three horizontal forces H_1, H_2, and $(H_1 - H_2)$, plus two vertical forces $V = \frac{\pm (H_1 h_1 - H_2 h_2)}{a}$.

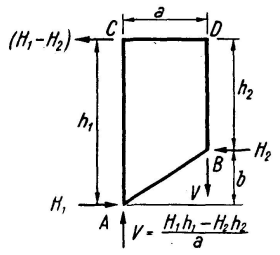

Fig. 1. Balanced set of external forces applied to a closed panel through its joints

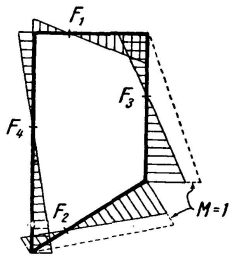

Fig. 3. Characteristic bending-moment diagram for a single closed panel

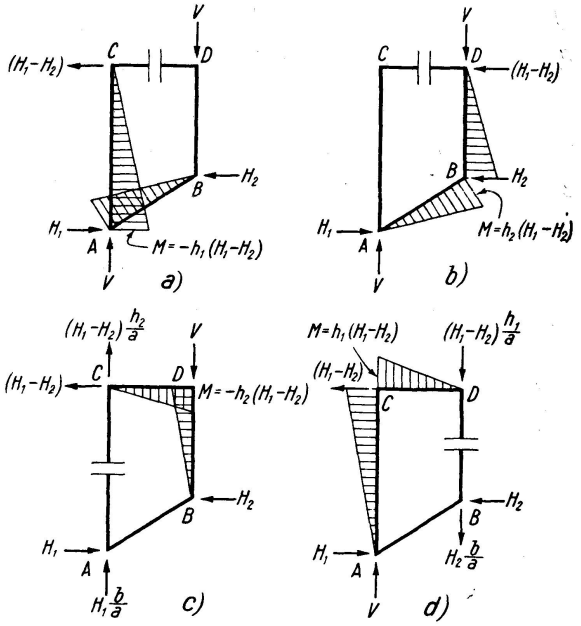

Fig. 2. Bending-moment diagrams for statically-determinate cases occurring with a single panel according to the position of the cut section

A cut section anywhere in the panel (Fig. 2) makes the system statically-determinate and the bending-moment diagram may then be reduced to any one of the forms shown in the figure by suitably choosing the position of the cut section and proportioning the amount of the vertical force V between the upper and lower panel points. If any one of these diagrams is selected, say Fig. 2b, and it is assumed that the moment M at the joint B is unity, it may easily be shown by column analogy, using the bending-moment diagram in the statically-determinate case as an elastic loading, that the bending-moment diagram for the closed panel has the shape shown in the shaded diagram (Fig. 3). Since the statical bending-moment diagram refers to any balanced set of external forces applied at the joints, it follows that the form of the bending-moment diagram for the closed panel must also refer to any such balanced set of forces; in other words, the latter is what might be termed a characteristic bending-moment diagram for the panel. As the values in this diagram are obtained on the basis of unit M at the joint B in the statically-determinate case, it is clear that, by finding the actual value of M corresponding to any given set of external forces, the true bending-moment diagram for the closed panel may be obtained by proportion from the characteristic bending-moment diagram; this characteristic bending-moment diagram should, therefore, always be associated with the relevant statical bending-moment diagram, shown dotted in Fig. 3. It follows from the above that points F_1, F_2, F_3 and F_4 in the figure are fixed points at which the bending moment due to any system of external

forces applied at the joints will always be zero, it being understood that these external forces are in equilibrium.

The elastic constants for a single closed panel may be readily found by using the following equations[5])

$$\bar{S} = \bar{S}_1 + \bar{S}_2 \tag{1a}$$

$$\bar{x} = \frac{\bar{S}_1 \bar{x}_1 + \bar{S}_2 \bar{x}_2}{\bar{S}} \tag{1b}$$

$$\bar{y} = \frac{\bar{S}_1 \bar{y}_1 + \bar{S}_2 \bar{y}_2}{\bar{S}} \tag{1c}$$

$$I_x = (I_{x_1} + I_{x_2}) + (\bar{S}_1 y_1^2 + \bar{S}_2 y_2^2) \tag{1d}$$

$$I_y = (I_{y_1} + I_{y_2}) + (\bar{S}_1 x_1^2 + \bar{S}_2 x_2^2) \tag{1e}$$

$$I_{xy} = (I_{xy_1} + I_{xy_2}) + (\bar{S}_1 x_1 y_1 + \bar{S}_2 x_2 y_2) \tag{1f}$$

which give the elastic constants for the resultant of any two members connected together in series, in terms of those for the separate members.

Virtual and Partial Equivalent Systems

These are illustrated in Fig. 4b, where the virtual equivalent system is represented by an elastic area PQ having rigid arms PB and QD which link it to joints B and D respectively; the elastic centre O of PQ is so located with respect to joints B and D that the relative displacements of these two points are the same for the virtual equivalent systems as for the panel. This virtual equivalent system may be used in replacement of all the members of the open-spandrel arch shown in dotted lines in Fig. 4b, including the real member DB.

The above virtual equivalent system when connected to the real deck member CD and the real arch rib member AB, constitutes a partial equivalent

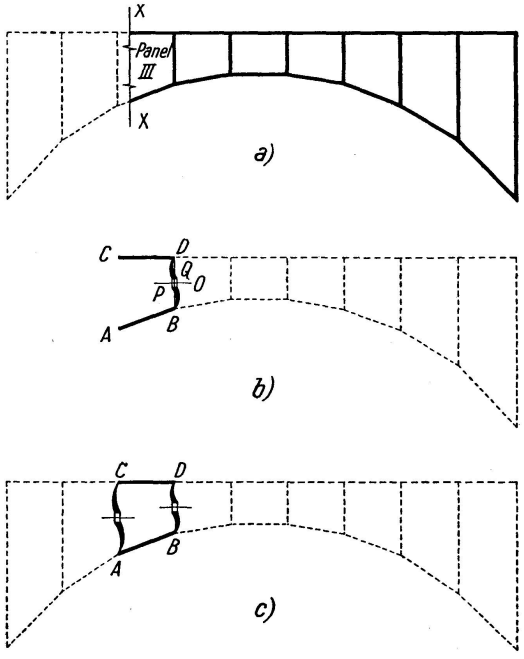

Fig. 4. (b) is a partial equivalent system for the part of the open-spandrel arch to the right of section XX (a); (c) is an equivalent panel based on panel III

[5]) Beaufoy and Diwan, "Equivalent Elastic Systems in the Analysis of Continuous Structures", Concrete and Constructional Engineering, November and December, 1950.

system based on panel III, and this may be used in replacement of all the members of the arch system to the right of section XX (Fig. 4a). The elastic constants of partial equivalent systems, as for single closed panels, may be obtained by applying equations (1).

Reference should be made to the earlier paper[6]) for further information about the properties of virtual and partial equivalent systems.

Equivalent Panel

An equivalent panel is illustrated in Fig. 4c by $ABCD$, where AB and CD are real members linked in a closed circuit to a virtual equivalent system on the left and one on the right, which replace the members shown in dotted lines. The elastic constants for such a panel may be obtained as for a single closed panel. In comparing the equivalent panel with the single closed panel it should be realised that the external forces at the joints of the equivalent panel are provided by the conjugate forces in the open-spandrel arch system, i.e., by the interaction between the panel considered and those on either side of it.

A characteristic bending-moment diagram can also be obtained as for a single closed panel; this gives the primary moments in the real members, i.e., the top and bottom chords. The primary moments in any equivalent panel induce moments in all panels to either side and so create moments throughout the structure. The determination of the induced moments follows from the relative displacements of the upper and lower ends of the posts[7]).

The diagram of primary and induced moments gives what may be termed a full characteristic bending-moment diagram for the whole open-spandrel arch system, based on the panel to which the primary moments refer. This diagram would be produced by applying a tensile or compressive force along the line of the diagonal of the equivalent panel of such a value that the force multiplied by the perpendicular distance was unity.

An end panel of an open-spandrel arch is usually subject to an external moment acting at one of the lower points so that the statical bending-moment diagram is generally trapezoidal over the arch-rib segment. To deal with this case, a second characteristic bending-moment diagram is necessary for the panel, and this follows from a statical bending-moment diagram having a rectangular part along the arch-rib segment similar to that shown in Fig. 5d. Each internal panel therefore has only one characteristic bending-moment diagram, but each end (or external) panel has two: the first of these is derived from a statical bending-moment diagram similar to that for the internal panels and will be referred to here as case A; the second arises when an external moment is applied to one of the joints of the panel, usually that on the lower chord, and

[6]) Beaufoy, op. cit.

[7]) Ibid., step (6).

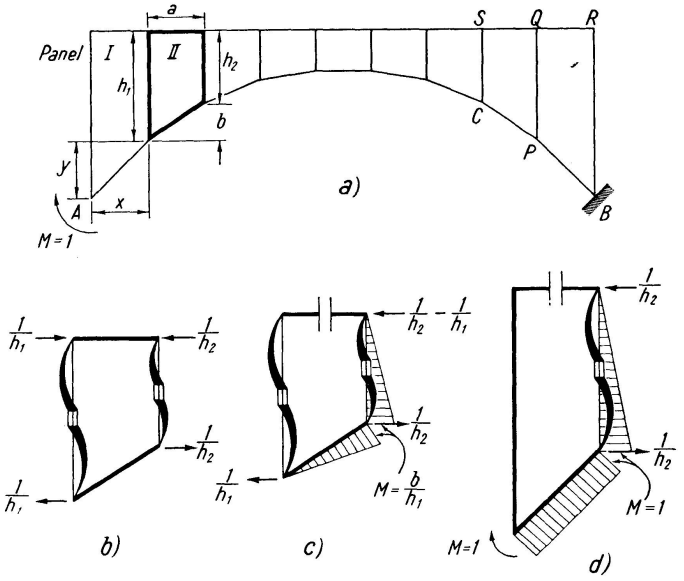

Fig. 5. (a) Open-spandrel arch: determination of elastic constants; (b) conjugate forces in internal equivalent panel II corresponding to unit M at end A; (c) statical bending-moment diagram, internal equivalent panel II; (d) conjugate forces and statical bending-moment diagram, external equivalent panel I

is derived from the statical bending-moment diagram for the case (case B). Any shape of bending-moment diagram in the main system for the external panels can then be readily obtained from the two conditions of loading, cases A and B. When an expansion joint is introduced in the deck the panels on either side of that containing the expansion joint must similarly be treated as if they were external panels.

There will, therefore, be one full characteristic bending-moment diagram for each internal panel and two full characteristic bending-moment diagrams for each external panel. This information is best collected together in tabular form.

The Whole Arch System

Elastic Constants

First consider a fixed-ended arch member AB. Release the end A and assume a unit moment M to be applied there; a reaction at B of $M=1$ will result. It can then easily be shown[8]) that the end A moves through distances

$$\phi = \bar{S} \tag{2a}$$

$$\Delta = -\phi \cdot \bar{y} \tag{2b}$$

and

$$\lambda = \phi \cdot \bar{x} \tag{2c}$$

from which the elastic constants $\bar{S}$, $\bar{x}$ and $\bar{y}$, for the arch member may be found.

[8]) Beaufoy and Diwan, "Analysis of Continuous Structures by the Stiffness Factors Method", Quarterly Journal of Mechanics and Applied Mathematics, vol. II, pt. 3, 1949.

Next, apply only a horizontal force $H=1$ at the end O of a rigid arm $A\,O$, O being at the elastic centre. Then, values of I_x and I_{xy} may be obtained from the following equations

$$I_x = \Delta \tag{2d}$$
$$I_{xy} = -\lambda \tag{2e}$$

In the symmetrical case, $I_{xy}=0$. Similarly, by applying only $V=1$ at O,

$$I_y = \lambda \tag{2f}$$

Thus, the remaining elastic constants I_x, I_y, and I_{xy} for the arch member are found.

Now, in the case of the open-spandrel arch, the deflection of a point P in the arch rib (Fig. 5a) may be obtained from the arch rib PB alone due to the bending moments on it, or from the members BR, RQ, QP due to the bending moments on them. Similarly, the deflection of the point C may be obtained by considering only the arch rib BPC, rather than members $BRQSC$. Hence, the deflections of points in the lower chord are obtained by considering the arch rib only, subject to the moments acting thereon. Thus, the deflections of end A may be found and subsequently transformed into elastic constants by applying equations (2). In passing, it should be observed that vertical deflections of corresponding points on the deck and arch rib are the same, disregarding axial deformations, but that horizontal and rotational displacements are not the same.

The above process will now be considered in more detail as it applies to the open-spandrel arch shown in Fig. 5a. Fix end B and apply unit moment at end A. Then, for the equivalent panel II, the conjugate forces corresponding to unit M at A are as shown in Fig. 5b. When the forces at the joints of the upper chord are combined into one force, Fig. 5c is obtained, and if the upper chord is assumed to be cut, a statical bending-moment diagram results similar to that shown in Fig. 2b but with a value for M of b/h_1. The characteristic bending-moment diagram for the panel was based on a unit value for M and the moments induced on either side followed from the characteristic bending-moment diagram. In the case of the equivalent panel, however, the value of M is not unity but b/h_1, viz., a coefficient C obtained from the proportions of the panel; it follows that the values in the characteristic bending-moment diagram and the moments induced to either side must all be multiplied by C.

For the special case of equivalent panel I, the conjugate forces are as shown in Fig. 5d, which also shows the statical bending-moment diagram, from which the characteristic bending-moment diagram may be derived. Thus, for unit M applied at end A, the coefficient $C=b/h_1$ for all internal panels, but $C=1$ for case B of the external panel (case A of the external panel does not arise). Each full characteristic bending-moment diagram is now multiplied by the corresponding C value to give actual primary and induced moments. The

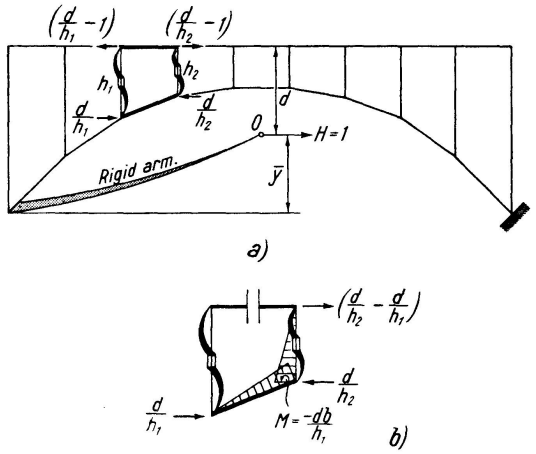

Fig. 6. (a) Conjugate forces on internal equivalent panel corresponding to unit H at the elastic centre O of an open-spandrel arch; (b) statical bending-moment diagram

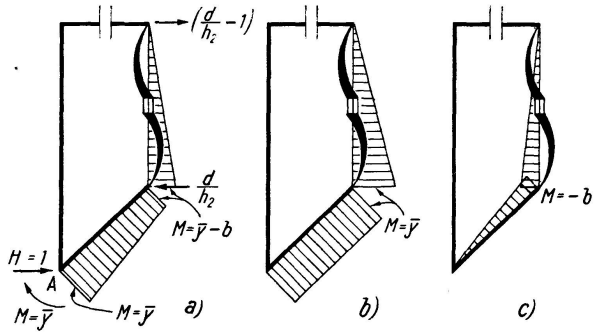

Fig. 7. (a) Conjugate forces and statical bending-moment diagram for external equivalent panel corresponding to unit H at the elastic centre of an open-spandrel arch. The statical bending-moment diagram may be broken down into the separate diagrams (b) and (c) due to M and H respectively

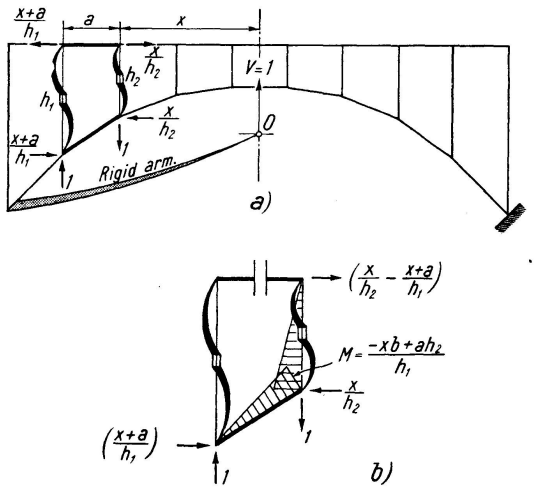

Fig. 8. (a) Conjugate forces on internal equivalent panel corresponding to unit V at the elastic centre O; (b) statical bending-moment diagram

summation of all values for the different panels will give the final bending-moment diagram for unit M. From this final bending-moment diagram the values of the elastic constants $\bar{S}$, $\bar{x}$ and $\bar{y}$ are found by substitution in equations (2). As this final bending-moment diagram for the whole structure must always diminish towards the crown, it follows that, compared with the same arch rib without the superstructure, the total elastic area $\bar{S}$ must be reduced, and the elastic centre must drop towards the springing line, that is, $\bar{y}$ must be smaller.

Next apply unit H only at the elastic centre O (Fig. 6a). Considering any internal equivalent panel, the conjugate forces and the statical bending-moment diagram will be as shown in Fig. 6b, so that for all internal panels the value of the coefficient C is $-d\,b/h_1$. Fig. 7a shows the conjugate forces for an external equivalent panel (H is transferred to A through the rigid arm OA). A cut section in the upper chord gives rise to the statical bending-moment diagram indicated; this is compounded of Figs. 7b and 7c, which refer respectively to the diagrams for M and H, and which are of forms already familiar, Fig. 7b being similar to Fig. 5d and Fig. 7c to Fig 2b. Thus, the coefficient for the characteristic bending-moment diagram in case A (Fig 7c) is $C = -b$, while for case B (Fig. 7b), $C = \bar{y}$. These values of C are now applied, as in the case of unit M, to the full characteristic bending-moment diagram to obtain a final bending-moment diagram for unit H by summation. From this final bending-moment diagram, the horizontal displacement Δ at point A is calculated and hence the value I_x is known from equation (2d).

Finally, apply unit V at point O (Fig. 8a). For an internal equivalent panel (Fig. 8b) it can be shown that

$$M = \frac{x\,b - a\,h_2}{h_1},$$

which may be plus or minus according to values. Hence the C value is

$$\frac{-x\,b + a\,h_2}{h_1}.$$

For an external equivalent panel the conjugate forces are as shown in Fig. 9. The shape of the statical bending-moment diagram is illustrated in Fig. 7a, and can similarly be reduced to forms corresponding to Figs. 7b and 7c, from which values of C are

$$\text{case A: } C = a,$$
$$\text{case B: } C = -L/2.$$

Hence, from these values of C, the final bending-moment diagram for unit V and the vertical displacement $\lambda_A = I_y$ are found, completing the determination of the elastic constants for the whole structure. For convenience of reference, the various values of C derived above are collected together in Table 1.

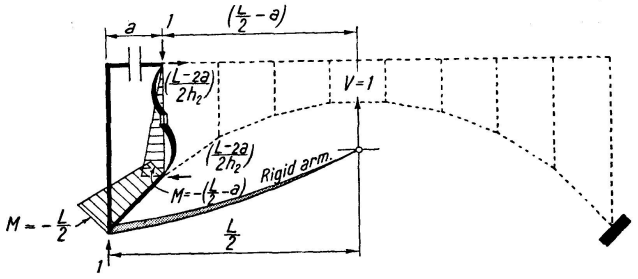

Fig. 9. Conjugate forces and statical bending-moment diagram for external equivalent panel corresponding to unit V at the elastic centre of an open-spandrel arch

Table 1. Values of the coefficient C for equivalent panels

Loading	Internal panel	External panel	
		Case A	Case B
Unit M	$\frac{b}{h_1}$	—	1.0
Unit H	$-\frac{d\,b}{h_1}$	$-b$	$\bar{y}$
Unit V	$\frac{-x\,b+a\,h_2}{h_1}$	a	$-\frac{L}{2}$

Stiffness Factors for the End A of the Whole Structure

These may be obtained from the elastic constants by substitution in the following equations[9]) which refer to the case when the arch is symmetrical and $I_{xy}=0$

$$m_\phi = \frac{1}{S} + \frac{\bar{y}^2}{I_x} + \frac{\bar{x}^2}{I_y}. \tag{3a}$$

$$h_\phi = \frac{\bar{y}}{I_x}\ [=m_\Delta]. \tag{3b}$$

$$v_\phi = \frac{-\bar{x}}{I_y}\ [=m_\lambda]. \tag{3c}$$

$$h_\Delta = \frac{1}{I_x}. \tag{3d}$$

$$v_\lambda = \frac{1}{I_y}. \tag{3e}$$

$$h_\lambda = 0. \tag{3f}$$

$$v_\Delta = 0. \tag{3g}$$

[9]) Beaufoy, op. cit.

Influence Lines for the Fixed-end Reactions of the Whole Structure

A horizontal force of amount h_Δ at the elastic centre will, by definition, cause a unit horizontal movement only at A. The resulting deflection line is the influence line for H, and can be found from the bending-moment diagram corresponding to the force h_Δ, which is obtained by proportion from that already found for unit H. The influence line for V may be found similarly. To get that for M, apply horizontal and vertical forces h_ϕ and v_ϕ respectively at the elastic centre O, together with a moment $1/\bar{S}$ to cause unit rotation only at A. The influence line for M is then obtained as the summation of the following deflection lines (I) that due to h_ϕ at O, obtained by proportion from the influence line for H, since $h_\phi = \bar{y}.h_\Delta$; (II) that due to v_ϕ at O, obtained by proportion from the influence line for V, since $v_\phi = -Lv_\lambda/2$; (III) that due to $M = 1/\bar{S}$. The bending-moment diagram is obtained by proportion from that for unit M previously derived and the deflection line follows.

Method of Analysis

Structural Analysis

1. Determination, for each of the partial equivalent systems, of the bending-moment diagrams corresponding to unit relative displacement imposed at the cut ends.
2. Evaluation of the elastic constants for the virtual equivalent systems for successive groupings of panels working from left to right, and also from right to left if the open-spandrel arch is not symmetrical. In a symmetrical case, the two sets of evaluations will be similar.
3. Determination, for each equivalent panel, of the elastic constants and the primary moments, and the determination of all the moments induced both to the right and to the left of each of the equivalent panels.
4. Evaluation, for the whole arch system, of the elastic constants, the stiffness factors for the ends of the arch system at the springings, and the influence lines for the fixed-end reactions M, H and V.

Stress Analysis

5. Determination of the fixed-end reactions for the given loading from the influence lines for M, H, and V.
6. Evaluation, for each equivalent panel, of the conjugate forces, the statical bending-moment diagram and the coefficient C.
7. Determination of the final bending-moment diagram by summation.

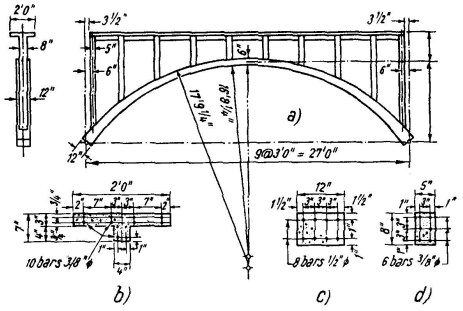

Fig. 10. Reinforced-concrete high-deck arch: (a) main dimensions; (b) section of deck; (c) section of arch rib; (d) section of post

Example

To illustrate the use of the method, it will now be applied to the solution of a 27-ft. span reinforced-concrete open-spandrel arch model[10]). The dimensions of this model, a high-deck arch without expansion joints, are shown in Fig. 10. For the purposes of the calculations, the effect of the joints will be disregarded, the analysis being based on a consideration of centre lines; this effect will not be of great importance owing to the absence of haunches. Furthermore, the arch rib between any two spandrel columns will be assumed prismatic with a constant cross section identical with that at the middle of its length. It would be possible to take into account the variation in the cross section of the arch rib but the differences involved would be slight. On the above basis, the values of the relative elastic areas ($\bar{S} \cdot 100 \cdot E$) of all members are as shown in Fig. 11.

Structural Analysis

Step 1. The elastic constants for all partial equivalent systems working from right to left, found by using equations (1), are collected together in Table 2, in which $\bar{x}$ and $\bar{y}$ are as measured from the upper left-hand end of the system. Then, for each partial equivalent system in turn, considering the lower left-hand end to be fixed, the forces required on the upper left-hand end to produce unit displacements there (viz., the stiffness factors for the upper

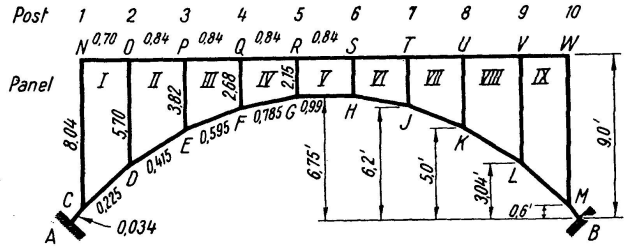

Fig. 11. Relative elastic areas for all members, as used in calculations

[10]) Wilson and Kluge, op. cit.

Table 2. Partial equivalent systems: elastic constants

Panel	II	III	IV	V	VI	VII	VIII	IX
$\bar{S}$	1.62	1.83	2.04	2.21	1.98	1.76	1.54	8.97
$\bar{x}$	1.84	1.82	1.80	1.76	1.77	1.78	1.78	2.37
$\bar{y}$	−1.68	−1.40	−1.21	−1.20	−1.24	−1.49	−1.79	−3.95
I_x	9.60	5.24	3.30	3.04	4.06	8.20	20.18	61.30
I_y	1.58	1.77	1.96	2.08	1.87	1.67	1.47	1.79
I_{xy}	0.14	0.19	0.14	0.05	−0.16	−0.35	−0.46	−2.67
I_x'	9.59	5.22	3.29	3.04	4.04	8.13	20.03	57.30
I_y'	1.58	1.76	1.96	2.08	1.86	1.66	1.45	1.67

ends relative to the lower ends) are found[11]); these values of m_Δ, h_Δ, v_Δ and m_ϕ, h_ϕ, v_ϕ are shown in Table 3. The values m_e and h_e shown in this table are found by transferring these forces to the elastic centre of the relevant virtual equivalent system and calculating the relative induced displacements (e. g. ϕ_Δ, Δ_Δ) of the upper end with respect to the lower end of the partial equivalent system[12]). Finally, for each partial equivalent system in turn, the bending-moment diagram is found by statics; these diagrams are collected together in Fig. 12.

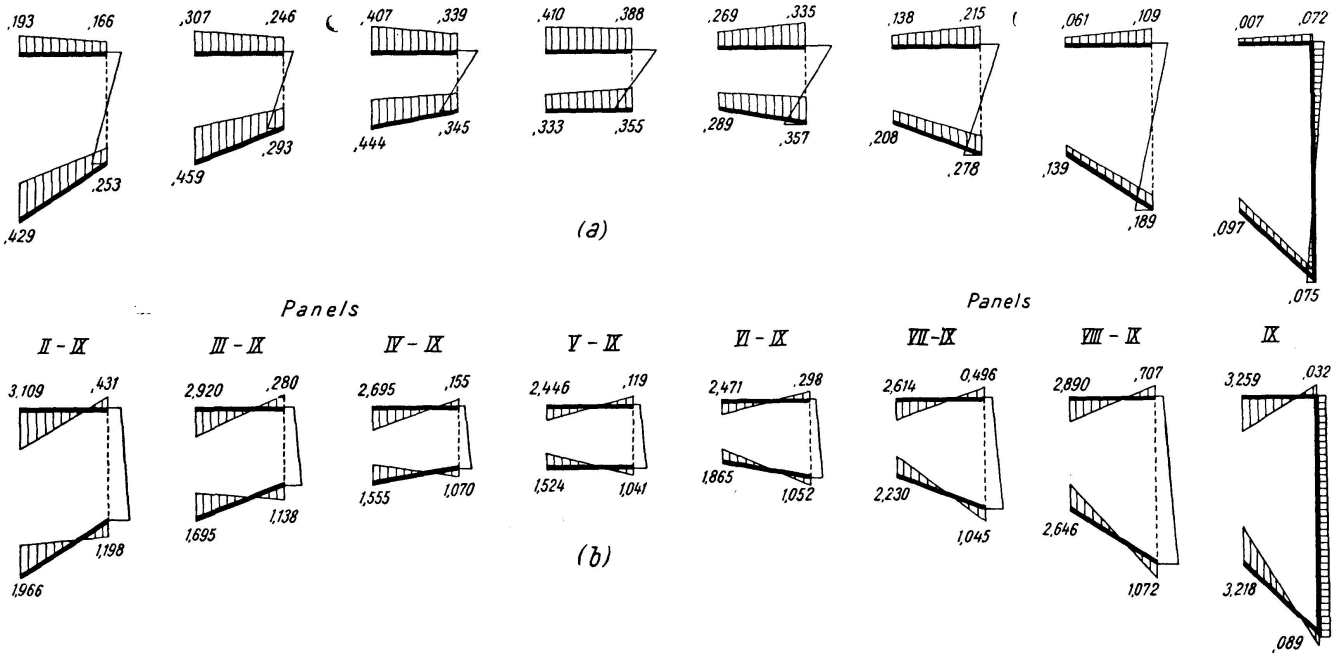

Fig. 12. Partial equivalent systems: (a) bending-moment diagram producing unit relative horizontal translation between upper and lower joints on left-hand side; (b) as for (a) but in respect of unit relative rotation

[11]) Beaufoy, op. cit., equation (4).

[12]) Beaufoy, op. cit., equation (5).

Table 3. Partial equivalent systems: stiffness factors and induced displacements of upper ends relative to lower ends

Panel	I	II	III	IV	V	VI	VII	VIII	IX
m_Δ	−0.193	−0.307	−0.407	−0.410	−0.269	−0.138	−0.061	−0.007	
h_Δ	0.105	0.192	0.304	0.330	0.248	0.124	0.050	0.018	
v_Δ	0.009	0.021	0.022	0.007	−0.022	−0.026	−0.016	−0.026	
m_e	—	0.023	0.020	0.010	0.018	0.000	0.012	0.011	
h_e	—	0.105	0.192	0.304	0.330	0.248	0.124	0.050	
ϕ_Δ	0.008	0.008	0.004	0.007	0.000	0.004	0.003	—	
Δ_Δ	0.283	0.230	0.215	0.236	0.353	0.510	0.660	—	
m_ϕ	3.109	2.920	2.695	2.446	2.471	2.614	2.890	3.259	
h_ϕ	−0.193	−0.307	−0.407	−0.410	−0.269	−0.138	−0.061	−0.007	
v_ϕ	−1.180	−1.067	−0.950	−0.855	−0.923	−1.040	−1.199	−1.320	
m_e	—	−0.777	−0.703	−0.623	−0.577	−0.661	−0.749	−0.853	
h_e	—	−0.193	−0.307	−0.407	−0.410	−0.269	−0.138	−0.061	
ϕ_ϕ	−0.287	−0.277	−0.258	−0.219	−0.232	−0.242	−0.243	—	
Δ_ϕ	−1.005	−0.731	−0.578	−0.546	−0.698	−1.000	−1.375	—	

Table 4. Virtual equivalent systems: relative actual stiffness factors and elastic constants

Panel	I	II	III	IV	V	VI	VII	VIII	IX
	Spandrel posts only								
$\bar{S}$	5.70	3.82	2.68	2.15	2.15	2.68	3.82	5.70	
m_ϕ	0.70	1.05	1.50	1.87	1.87	1.50	1.05	0.70	
h_ϕ	−0.18	−0.39	−0.80	−1.25	−1.25	−0.80	−0.39	−0.18	
h_Δ	0.06	0.20	0.58	1.12	1.12	0.58	0.20	0.06	
	Virtual equivalent systems								
M_ϕ	3.81	3.97	4.20	4.32	4.34	4.11	3.94	3.96	
H_ϕ	−0.37	−0.70	−1.21	−1.66	−1.52	−0.94	−0.46	−0.18	
H_Δ	0.16	0.39	0.88	1.45	1.36	0.70	0.25	0.08	
$\bar{S}$	0.34	0.37	0.39	0.42	0.38	0.35	0.32	0.29	
$\bar{y}$	−2.26	−1.80	−1.38	−1.15	−1.12	−1.35	−1.85	−2.39	
I_x	6.12	2.57	1.14	0.69	0.74	1.44	4.05	13.05	

Table 5. Equivalent panels: elastic constants

Panels	I and IX	II and VIII	III and VII	IV and VI	V
$\bar{S}$	9.30	1.91	2.15	2.39	2.59
$\bar{x}$	0.22 (I)	1.57 (II)	1.55 (III)	1.54 (IV)	1.50
	2.28 (IX)	1.43 (VIII)	1.45 (VII)	1.46 (VI)	
$\bar{y}$	−3.89	−1.79	−1.47	−1.22	−1.19
I_x	68.12	22.74	9.35	4.74	3.78
I_y	3.60	2.40	2.69	2.92	3.08
I_{xy}	3.96	0.44	0.41	0.22	0.00
I_x'	63.77	22.66	9.28	4.72	3.78
I_y'	3.37	2.39	2.66	2.92	3.08

Table 6. Equivalent panels: forces acting at elastic centre

Panel	I (Case B)	I (Case A)	II	III	IV	V
P	−35.3	−24.0	−37.3	−49.2	−60.5	0.0
M_x	156.2	114.7	123.7	90.4	76.5	0.0
M_y	−52.6	−45.6	−32.7	−41.5	−48.9	−53.0
M_x'	214.0	164.8	129.7	96.8	80.2	0.0
M_y'	−61.5	−52.2	−35.1	−45.5	−52.4	−53.0
M	− 3.8	− 2.6	−19.6	−22.9	−25.4	0.0
H	3.4	2.6	5.8	10.4	17.0	0.0
V	−18.3	−15.6	−14.7	−17.2	−18.0	−17.3

Table 7. Virtual equivalent systems: induced displacements of upper ends relative to lower ends

Panel	I (Case B)	I (Case A)	II	III	IV	V	VI
m_e	− 2.17	− 4.03	− 4.33	− 2.50	− 0.10	1.00	
h_e	−13.49	−14.27	−19.25	−25.30	−27.45	−22.25	
$\phi \rightarrow$	0.73	− 1.36	− 1.60	− 0.96	− 0.41	0.38	
$\Delta \rightarrow$	−80.55	−90.20	−52.30	−30.13	−19.47	−15.98	
m_e		− 0.05	− 0.28	0.22	1.00		
h_e		− 5.75	−10.42	−17.00	−22.25		
$\leftarrow \phi$		− 0.01	− 0.09	0.08	0.38		
$\leftarrow \Delta$		−75.03	−42.37	−24.27	−15.98		

Step 2. Values of the relative elastic areas ($\bar{S} \cdot 100 \cdot E$) and stiffness factors for the upper ends of spandrel posts are given in Table 4. The stiffness factors follow from the following relations

$$m_\phi = \frac{4}{\bar{S}}; \quad h_\phi = \frac{-6}{\bar{S} \cdot L}; \quad h_\Delta = \frac{12}{\bar{S} \cdot L^2}.$$

Each post in turn is then combined with the partial equivalent system on its right to give the corresponding virtual equivalent system, and values of the relative actual stiffness factors M_ϕ, H_ϕ, H_Δ (for the upper left-hand ends) follow by definition from the combination. Substitution of these values in the Table given in the earlier paper[13]) enables the elastic constants for the virtual equivalent systems to be found.

Step 3. The elastic constants of equivalent panels are next determined (Table 5). Then, assuming an arbitrary bending-moment diagram ($M = 100$) for the statically-determinate case, and applying column analogy, we get the elastic loads on the analogous columns and the moments of these loads (Table 6), from which the moment M and the forces H and V acting in each case at the elastic centre of the equivalent panel are found. These are also shown in Table 6, which includes cases A and B of the external panel I, and which deals only with the left-hand half of the structure, the values in the other half being symmetrical. From these values, the primary moments (Fig. 13) are calculated.

Transferring moments to the elastic centre of the virtual equivalent system on the right of an equivalent panel, we get the values of m_e and h_e in the first half of Table 7, from which follow the induced displacements ϕ and Δ

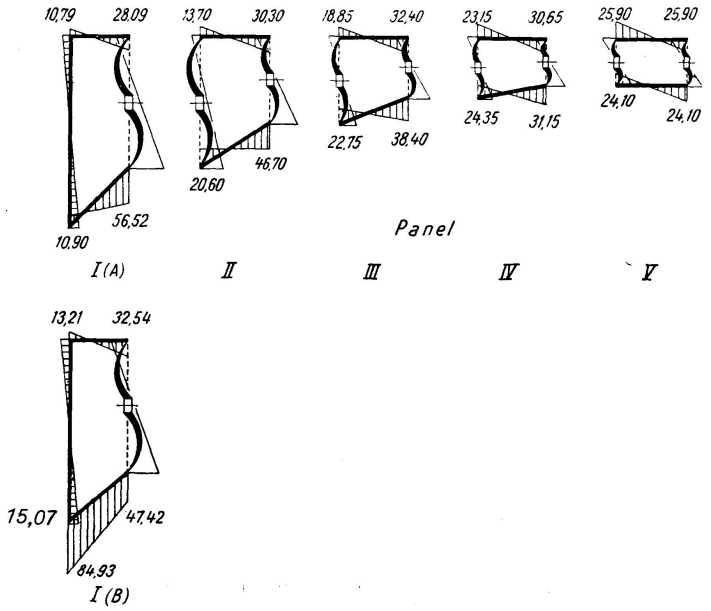

Fig. 13. Equivalent panels: primary moments

[13]) Beaufoy, op. cit.

Table 8. Induced displacements of upper

Post	2		3		4	
	ϕ	Δ	ϕ	Δ	ϕ	Δ
Panel I (A)	−1.36	−90.20	−0.36	−24.21	−0.09	− 5.28
Panel I (B)	0.73	−80.55	−0.88	−23.61	0.05	− 4.76
Panel II	−0.01	−75.03	−1.60	−52.30	0.02	−10.84
Panel III	−0.11	−27.50	−0.09	−42.37	−0.96	−30.13
Panel IV	−0.01	− 7.99	−0.11	−12.33	0.08	−24.27
Panel V	−0.01	− 1.93	−0.00	− 2.93	−0.09	− 5.96

Table 9. Induced moments (C = 1.0)

Loading on equiv. panel	I		II		III		IV	
(Deck)	*NO*	*ON*	*OP*	*PO*	*PQ*	*QP*	*QR*	*RQ*
I (case B)	−13.21	−32.54	17.77	−13.03	4.69	−6.00	2.08	−1.61
I (case A)	−10.79	−28.09	13.12	−15.49	6.38	−6.01	1.90	−1.81
II	−5.43	0.48	−13.70	−30.30	11.47	−13.30	4.46	−3.70
III	−2.01	−0.16	−4.66	2.33	−18.85	−32.40	9.70	−10.40
IV	−0.58	0.02	−1.42	0.44	−5.16	3.52	−23.15	−30.65
V	−0.14	−0.02	−0.32	0.18	−1.32	0.59	−5.24	5.22
(Arch)	*CD*	*DC*	*DE*	*ED*	*EF*	*FE*	*FG*	*GF*
I (case B)	84.93	−47.42	33.16	−21.27	12.29	−5.87	2.04	−1.71
I (case A)	−10.90	−56.52	41.38	−21.15	11.70	−6.64	2.49	−1.73
II	−5.60	7.32	−20.60	−46.70	26.70	−13.49	4.81	−3.74
III	−2.06	3.05	−7.91	6.12	−22.75	−38.40	14.90	−9.37
IV	−0.60	0.81	−2.22	2.01	−6.80	4.86	−24.35	−31.15
V	−0.14	0.22	−0.55	0.41	−1.57	1.44	−6.09	3.90

ends of posts relative to their lower ends

5		6		7		8		9	
ϕ	Δ	ϕ	Δ	ϕ	Δ	ϕ	Δ	ϕ	Δ
0.00	− 1.08	0.01	− 0.26	−0.00	−0.10	0.00	−0.05	−0.00	−0.03
−0.03	− 1.06	0.01	− 0.23	−0.00	−0.09	0.00	−0.04	−0.00	−0.03
−0.04	− 2.35	0.02	− 0.53	−0.01	−0.20	0.00	−0.10	−0.00	−0.06
0.12	− 5.94	0.01	− 1.46	−0.00	−0.53	−0.00	−0.27	−0.00	−0.17
−0.40	−19.47	0.22	− 4.35	−0.05	−1.71	0.01	−0.81	−0.00	−0.54
0.38	−15.98	0.38	−15.98	−0.09	−5.96	−0.00	−2.93	−0.01	−1.93

in deck members and arch rib

V		VI		VII		VIII		IX	
RS	*SR*	*ST*	*TS*	*TU*	*UT*	*UV*	*VU*	*VW*	*WV*
0.35	−0.41	0.10	−0.07	0.00	−0.02	0.00	−0.00	0.00	−0.00
0.45	0.42	0.09	−0.08	0.01	−0.02	0.00	−0.01	0.00	−0.00
0.86	−0.91	0.20	−0.17	0.01	−0.05	0.01	−0.01	0.00	−0.01
2.74	−2.28	0.43	−0.49	0.06	−0.12	0.01	−0.03	−0.00	−0.01
6.98	−7.59	1.72	−1.40	0.10	−0.39	0.06	−0.08	−0.01	−0.04
−25.90	−25.90	5.22	−5.24	0.59	−1.32	0.18	−0.32	−0.02	−0.14
GH	*HG*	*HJ*	*JH*	*JK*	*KJ*	*KL*	*LK*	*LM*	*ML*
0.40	−0.34	0.04	−0.10	0.03	−0.02	0.01	−0.01	0.00	−0.00
0.36	−0.39	0.06	−0.10	0.02	−0.02	0.01	−0.01	0.00	−0.00
0.84	−0.79	0.11	−0.22	0.06	−0.05	0.01	0.02	0.01	−0.01
1.79	−2.25	0.40	−0.54	0.12	−0.14	0.04	−0.05	0.02	−0.01
7.10	−6.48	0.85	−1.80	0.47	−0.42	0.10	−0.16	0.06	−0.04
−24.10	−24.10	3.90	−6.09	1.44	−1.57	0.41	−0.55	0.22	−0.14

of the upper relative to the lower ends of the virtual equivalent systems; these displacements propagate to the right to the other panels. The second half of this table similarly shows the displacements which propagate to the left. This propagation is shown in Table 8, which gives the displacements of upper ends of posts relative to their lower ends, as induced from the equivalent panels in turn, the values being obtained by proportion from those for the partial equivalent systems (Table 3). These values are now used in conjunction with the moments in Fig. 12 (which are for unit imposed relative rotations or translations) to prepare a table of induced moments (for unit C) in the deck members and the arch rib (Table 9) due to the arbitrary loading condition on the equivalent panel.

Step 4. Now assume two end moments $M = 100$ applied at the abutments in opposite directions. The values of the coefficient C for panels II, III and IV are 0.329, 0.30 and 0.197 respectively; these values, applied to the relevant figures in Table 9, give the actual primary and induced moments, which are plotted in Fig. 14a.

Table 10. Checks for statical equilibrium for the following loadings a) $M = 100$; b) $H = 100$; c) $V = 10$

Section just left of Post No.	2	3	4	5	6
a) Shear Q in post on left	3.97	6.90	10.42	12.20	6.18
Thrust T in deck $= \Sigma Q$	3.97	10.87	21.29	33.49	39.67
$T \cdot h$	23.70	43.48	59.50	75.20	89.10
Moment M_d in deck	32.42	22.22	19.42	12.60	5.74
Moment M_r in rib	43.95	34.46	21.03	12.22	5.17
$M_r + M_d + T \cdot h$	100.07	100.16	99.95	100.02	100.01
External moment	*100.00*	*100.00*	*100.00*	*100.00*	*100.00*
b) Shear Q in post on left	+1.72	−6.68	−28.11	−46.20	−26.75
Thrust T in deck $= \Sigma Q$	+1.72	−4.96	−33.07	−79.27	−106.03
$T \cdot h$	10.10	−19.84	−92.70	−178.40	−238.50
Moment M_d in deck	39.67	41.69	−63.50	−54.50	−24.85
Moment M_r in rib	36.28	−48.71	−73.84	−52.15	−21.89
$M_r + M_d + T \cdot h$	86.05	−110.24	−230.04	−285.05	−285.24
External moment	*−86.00*	*110.00*	*230.00*	*285.00*	*285.00*
c) Shear Q in post on left	3.78	4.91	3.56	−2.21	−10.05
Thrust T in deck $= \Sigma Q$	3.78	8.69	12.25	10.05	0
$T \cdot h$	22.50	34.80	34.30	22.60	0
Moment M_d in deck	35.10	14.78	5.41	−3.61	0
Moment M_r in rib	47.02	25.45	5.24	−4.00	0
$M_r + M_d + T \cdot h$	104.62	75.03	44.05	14.99	0
External moment	*−105.00*	*−75.00*	*−45.00*	*−15.00*	*0*

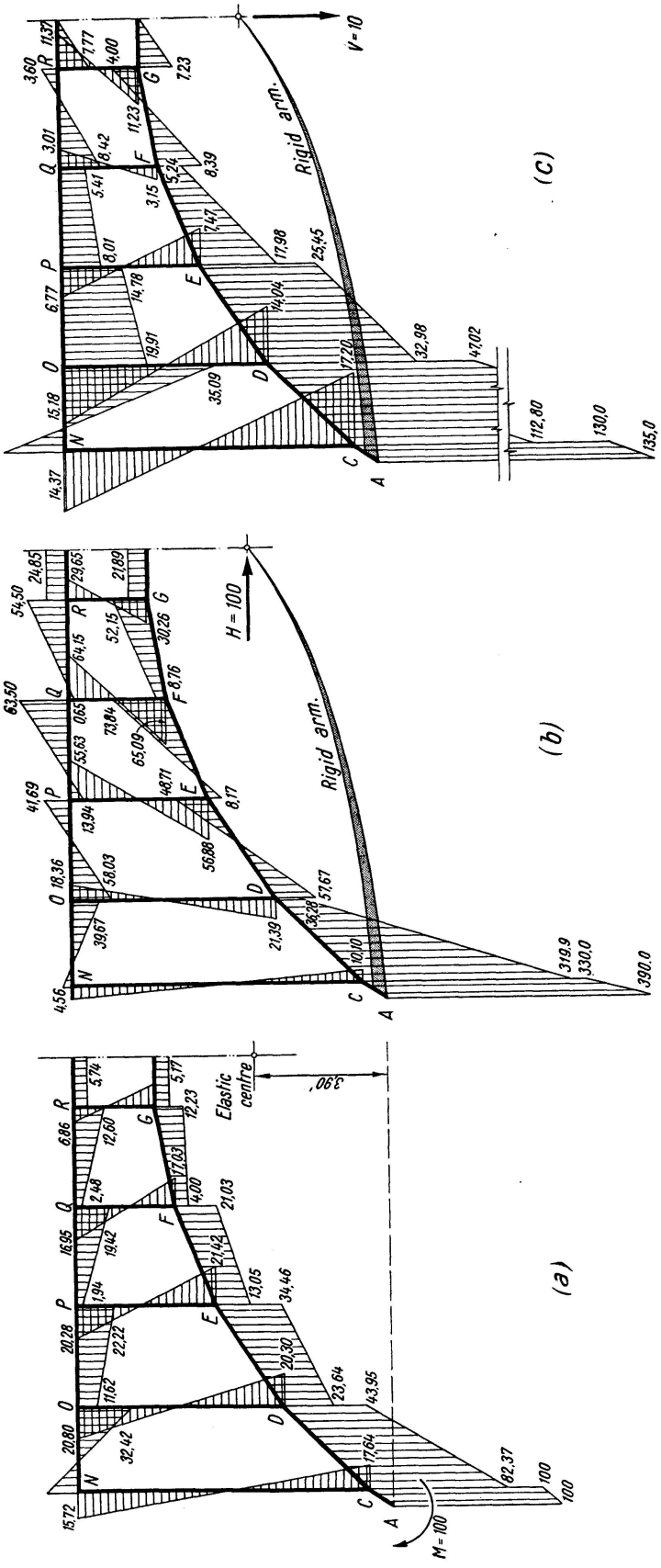

Fig. 14. Bending-moment diagrams for the following cases: (a) two end moments $M = 100$ applied at the abutments in opposite directions; (b) horizontal force $H = 100$ applied at the elastic centre; (c) vertical force $V = 10$ applied at the elastic centre

The deflection line for the arch rib, assuming a trapezoidal bending-moment diagram in each arch segment between two spandrel posts, may be obtained by the moment-area method; values of the horizontal and vertical displacements Δ and λ respectively of points on the arch rib relative to the tangent to the rib at the crown are shown in Table 11a. Since the deflection line drawn from these values is due to an end moment $M = 100$, it follows from equation (2a) that the total elastic area $\bar{S}$ for the whole system with reference to A and B is

$$\frac{97.54}{100} = 0.975,$$

while, from equation (2b), the height $\bar{y}$ of the elastic centre above the springing line $A\,B$ is

$$\frac{190.5}{48.77} = 3.90 \text{ ft.}$$

The deflection line can also be obtained relative to the tangent to the rib at the end B; the values are given in the Table.

Hence, from equation (2c), the horizontal distance $\bar{x}$ of the elastic centre from the end A is

$$\frac{1316.8}{97.54} = 13.5 \text{ ft.}$$

which conforms to the requirements of symmetry.

Now that the position of the elastic centre has been determined, consider a horizontal load $H = 100$ to act on the arch through its elastic centre and through a rigid arm connected to end A. The coefficients C for the internal panels, by which the moments in Table 9 have to be multiplied, are -1.63, -1.5, and -1.005 for panels II, III and IV respectively. For external panel I, the statical bending-moment diagram over $C\,D$ is trapezoidal with values of $M_C = 330$ and $M_D = 86$. The panel may, therefore, be considered as subject to a case A loading with $M = -244$ or $C = -2.44$ plus a case B loading with $M = 330$ or $C = 3.30$. The resulting bending-moment diagram is shown in Fig. 14b.

Deflections relative to the tangent at the crown are given in Table 11b. Since the force H acts through the elastic centre, the inclination of the end tangent relative to the tangent at the crown is zero. The displacement of end A relative to end B is, therefore, a pure horizontal translation Δ of amount

$$2 \cdot 279.2 = 558.4.$$

Hence, from equation (2d),

$$I_x = \frac{558.4}{100} = 5.584.$$

Consider next a vertical load $V = 10$ acting downwards on the system through the elastic centre, which is rigidly connected to end A. The coefficients

Table 11. Deflection lines for M, H and V

Point	*A*	*C*	*D*	*E*	*F*	*G*	Crown	*H*	*J*	*K*	*L*	*M*	*B*
a) Deflections for $M = 100$, relative to tangent at crown													
ϕ	48.77	45.37	31.17	19.07	8.92	2.56	0						
Δ	−190.5	−162.3	−70.76	−20.72	−3.46	0	0						
λ	257.85	234.32	140.42	63.91	20.75	1.92	0						
Deflection line, relative to tangent at end *B*													
ϕ	97.54	94.14	79.94	67.84	57.69	51.33	48.77	46.21	39.85	29.7	17.6	3.4	0
λ	1316.8	1258.8	1053.1	830.45	641.03	475.9	400.8	329.58	202.10	98.9	28.9	0.85	0
b) Deflections for $H = 100$, relative to tangent at crown													
ϕ	0	−12.30	−52.30	−54.17	−34.62	−10.8	0						
Δ	−279.2	−275.6	−183.9	−72.1	−14.10	0	0						
λ	−490.7	−487.7	−401.02	−230.26	−84.9	−8.1	0						
Deflection line, relative to tangent at end *B*, corresponding to unit horizontal translation, viz. influence line for fixed-end thrust *H*													
λ	0	0.005	0.161	0.467	0.728	0.8655	0.879						
Experimental value	*0*		*0.164*	*0.463*	*0.764*	*0.896*							
c) Deflections for $V = 10$, relative to tangent at end *B*													
ϕ							44.96	43.16	41.44	34.54	22.42	4.5	0
λ	−872.4	−871.27	−834.5	−748.2	−632.05	−502.79	−436.2	−369.61	−240.35	−124.2	−37.90	−1.13	0
Deflection line, relative to tangent at end *B*, corresponding to unit vertical translation, viz., influence line for fixed-end reaction *V*													
λ	1.00		0.956	0.857	0.723	0.576		0.424	0.277	0.143	0.044		0
Experimental value	*1.00*		*0.954*	*0.862*	*0.728*	*0.578*		*0.422*	*0.272*	*0.138*	*0.046*		*0*
d) Influence line for fixed-end moment *M*													
λ for $m = 1.03$	13.50		10.85	8.55	6.6	4.9		3.394	2.08	1.018	0.298		0
λ for $h = 0.7$	0		0.628	1.822	2.84	3.38		3.38	2.84	1.822	0.628		0
λ for $v = -0.155$	−13.50		−12.92	−11.59	−9.80	−7.80		−5.73	−3.72	−1.93	−0.587		0
Total λ	0		−1.44	−1.22	−0.36	0.48		1.04	1.20	0.91	0.34		0
Experimental value	*0*		*−1.42*	*−1.28*	*−0.30*	*0.55*		*1.17*	*1.37*	*0.99*	*0.34*		*0*

C for the loading of internal panels II, III, IV and V are 0.0453, -0.075, -0.212, and -0.30 respectively; the signs of these quantities for corresponding panels on the right of the crown are reversed.

The statical bending-moment diagram for the external panels is trapezoidal along the rib segments CD and LM, and may be considered as subject to a case B loading with $M_c = 130$ or $C = 1.30$, plus a case A loading with $M_D = -25$ or $C = -0.25$. Fig. 14c shows the bending-moment diagram.

Deflections relative to the tangent at the fixed end B are shown in Table 11c. At end A, the deflection λ is -872.4 so that, from equation (2f), the vertical displacement I_y due to $V = 1.0$ at the elastic centre is 87.24. The elastic constants for the open-spandrel arch are now determined. They are: $\bar{S} = 0.9754$; $\bar{x} = 13.5$; $\bar{y} = 3.90$; $I_x = 5.584$; $I_y = 87.24$; from equation (2e) it can be seen that $I_{xy} = 0$. From these values, the stiffness factors for the end A are readily found, by substitution in equations (3), to be: $m_\phi = 5.846$; $h_\phi = 0.70$; $v_\phi = 0.155$; $h_\Delta = 0.179$; $v_\lambda = 0.0115$.

Influence lines for the fixed-end reactions are calculated by proportion from the deflection lines (Table 11). Thus, that for H is obtained as the deflection line, relative to the fixed ends A and B, due to the application at the elastic centre of a force $h_\Delta = 0.179$ which will produce only a unit horizontal translation at the end A. The ordinates of this influence line are given in the Table at (b). Similarly, a vertical force of $v_\lambda = 0.0115$ at the elastic centre produces a deflection line which is the influence line for V at the abutment (Table 11c).

To produce a pure rotation of unit amount at the springing A, the necessary forces at the elastic centre are:

$$m_0 = \frac{1}{\bar{S}} = 1.026,$$

$$h_0 = \frac{\bar{y}}{I_x} = 0.70, \quad \text{and}$$

$$v_0 = \frac{-\bar{x}}{I_y} = -0.155.$$

From the bending-moment diagrams and deflection lines obtained for the three cases of loading M, H and V, the total bending-moment diagram and deflection line due to m_0, h_0 and v_0 applied simultaneously can be readily obtained by summation. This deflection line is the influence line for the fixed-end moment at the abutment A (Table 11d). The bending-moment diagram due to an imposed rotation $\phi = 10.0$ at the end A is given in Fig. 15.

The influence lines calculated above are compared in Table 11 with those obtained experimentally[14]); in Fig. 16 they are plotted, and the calculated influence lines for the arch rib only, which are also shown, indicate the extent of the participation of the deck.

---

[14]) Wilson and Kluge, op. cit.

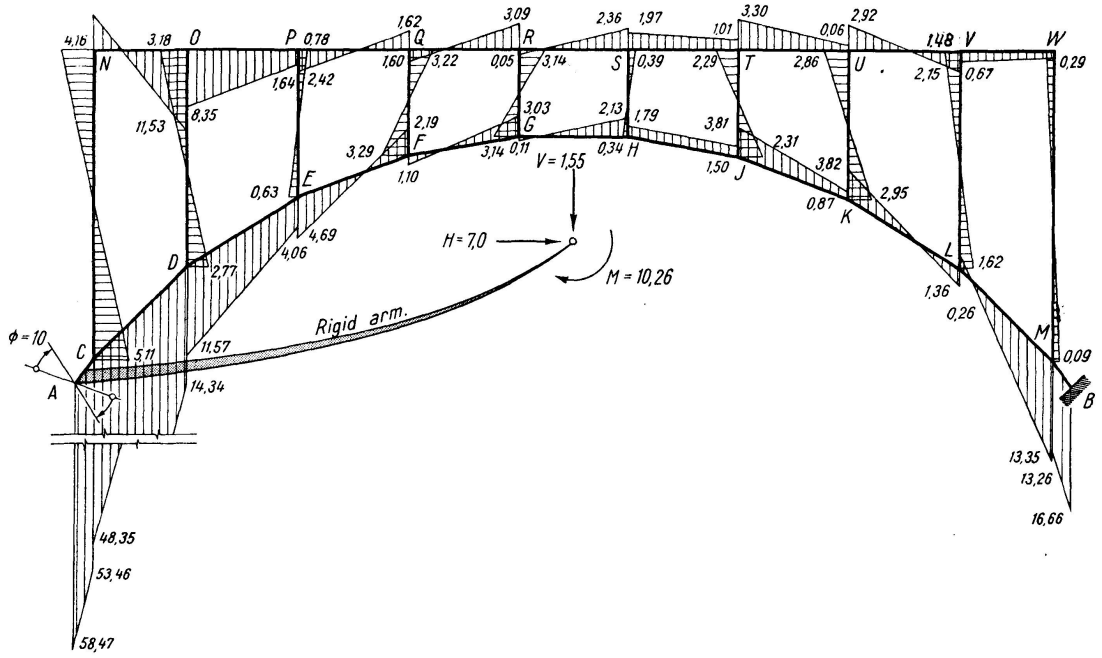

Fig. 15. Bending-moment diagram produced by pure unit rotation of free end A (end B fixed)

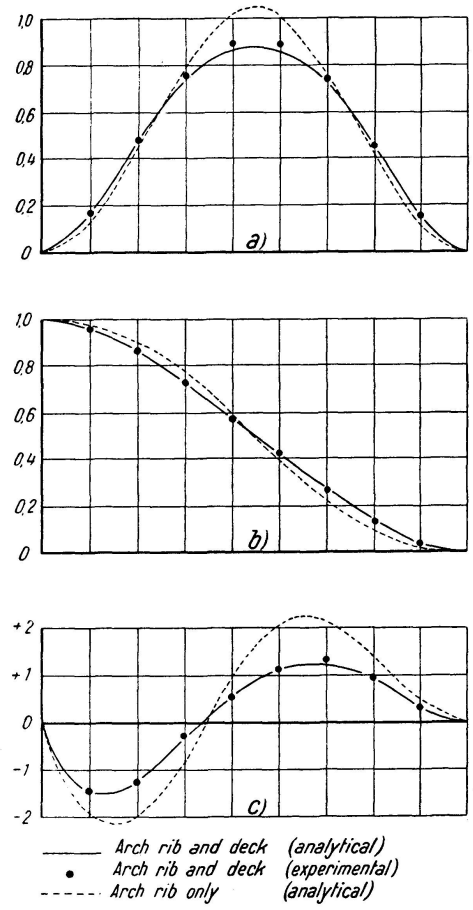

Fig. 16. Calculated and experimental influence lines for fixed-end reactions (a) for H; (b) for V; (c) for M. Calculated influence lines for the arch rib only are shown in dotted lines

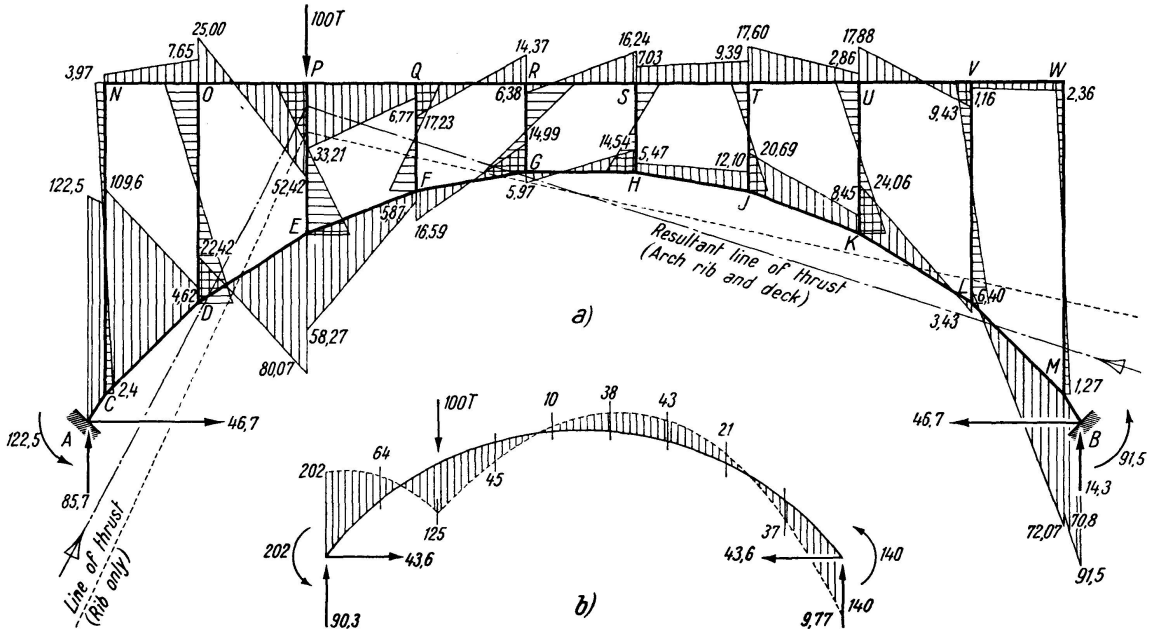

Fig. 17. Bending-moment diagram (a) for given loading case compared (b) with that for arch rib only

Stress Analysis

The effect of a particular case of loading on the structure, viz. a concentrated load of 100 tons at point P (Fig. 17) will now be considered.

Step 5. From the influence lines, the fixed-end reactions due to the applied load are found; they are indicated on Fig. 17.

Step 6. For each equivalent panel, the statical bending-moment diagram is determined from the loading condition under consideration and this fixes the value of the coefficient C for the panel. For internal panels, if M_1 and M_2 (Fig. 18) are the moments of all forces to one side about the two lower joints, M_2 being about the joint nearer to the centre of span and the signs being as shown in the figure, the coefficient C is

$$\frac{M_2 h_1 - M_1 h_2}{100 \cdot h_1},$$

in which the factor 100 appears in order to correct for the fact that the characteristic bending-moment diagram previously obtained was for $M = 100$. For the two external panels the bending-moment diagram for the main system is divided into a triangle and a rectangle, as previously stated. The values of C for the different panels are listed in Table 12.

Step 7. These values of C are now applied in turn to the moments shown in Table 9, which are for unit C, and the proportionate moments for each

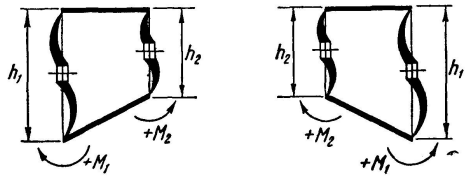

Fig. 18. Signs used in deriving the coefficient C for an internal equivalent panel in the stress analysis

Table 12. Values of the coefficient C for the various equivalent panels when a load of 100 tons is applied at point P

Panel	C	Panel	C
I (case B)	−1.072	VI	0.036
I (case A)	0.995	VII	−0.304
II	1.635	VIII	−0.512
III	−0.516	IX (case B)	0.708
IV	−0.567	IX (case A)	−0.788
V	−0.430		

panel are then summed to give the total moments, shown graphically in Fig. 17a, which is the bending-moment diagram for the assumed loading case. The resultant line of thrust for the arch rib and deck and for the arch rib only without a deck are shown in the figure, while the corresponding bending-moment diagram for an arch rib only is also given for comparison in Fig. 17b.

Checks and Comment on the Analysis

Checks will now be made on the calculations, which were all performed by slide rule, in order to demonstrate their self-consistency. First consider the bending-moment diagram for end moments of $M = 100$ (Fig. 14a). For any vertical section cutting both the deck and the arch rib the sum of the moments of the internal stresses, including both forces and moments, in the two cut sections about any point along the vertical section must be equal to the moment $M = 100$. Taking moments about the point of intersection of this vertical section with the arch rib the following expression must apply

$$M_r + M_d + T \cdot h = 100$$

where M_r is the moment in the rib, M_d the moment in the deck, T the thrust in the deck, and h the distance between the two points of intersection of the vertical section with the arch rib and deck. Appropriate signs have to be employed in this equation. The thrust T in the deck is readily obtained as the sum of the shearing forces in the spandrel columns on either side. Taking the vertical sections just to the left of the spandrel columns the sum of these moments is as in Table 10a, which reveals an interesting fact. A great part of the externally-applied moment is resisted by the thrust transmitted to the deck through the spandrel columns. As we move towards the centre of the arch, this part becomes the most important one in resisting the moment, the value it contributes increasing from 23.7% in the first panel up to nearly 90% of the whole moment in the middle panel.

Next, consider the bending-moment diagram for $H = 100$ (Fig. 14b), where the moments of the internal forces on any vertical section about its intersection

with the arch rib must balance the moment of the external force $H = 100$ (Table 10b). It will be seen that the greater part of the external moment is balanced by the thrust transmitted to the deck through the spandrel columns; at the central panel this part amounts to about 84% of the total moment. It will also be seen that the moments produced in the spandrel columns are large; in the internal panels they are of the same order of magnitude as the moments produced in both the arch rib and the deck. The spandrel columns are, however, of much smaller section. Furthermore, the thrust produced in the deck is very high. In those panels in which the resultant line of thrust (that of the x-axis through the elastic centre) falls inside the panel, the thrust in the deck reduces the thrust in the arch rib and in that way assists the rib. Towards the centre, however, where the resultant line of thrust falls outside the panels, this thrust acts in the same direction as the external force $H = 100$, and so the thrust in the arch rib is increased. Thus, in the central panel, in which the deck is in tension, $T = 106.03$, a higher value even than that of the external force. It will be seen that the thrust at the crown in the arch rib $= 100 + 106.03 = 206.03$. The thrust in the deck, then, does not always assist the rib; a fact which becomes of importance in a consideration of shrinkage and temperature stresses.

The check for statical equilibrium in the case of $V = 10$ is similarly given in Table 10c.

The effect of deck participation for this particular case of loading may now be studied. First, it will be seen (Fig. 17) that the line of thrust has moved closer to the springings A and B, thereby reducing the fixed-end moments by as much as 40% at A and 36% at B. At these ends, the fixed-end moments are totally resisted by the arch rib; the reduction is therefore of great value. In the external panels, also, the contribution of the deck to the resistance to external moments is small, indeed almost negligible, owing to the very small shearing forces in the columns; but these external moments are already reduced by 40% and 36% by the deck participation which brought the line of thrust nearer to the arch rib in these panels. On the other hand, this reduction in the fixed-end moments gives rise to an increase in both the positive and the negative moments in the internal panels, where the resultant line of thrust is moved further from the arch rib, as shown in Fig. 17a. In these panels, however, there is an important item to be taken into account, which, together with the moments already transmitted to the deck, greatly relieves the moments in the arch rib; this item is the thrust transmitted to the deck through the shear in the spandrel columns. Thus, at J in the arch rib (Fig. 17b) the moment on the arch rib only is 43. In the open-spandrel arch the moment in the deck is 17.6 (Table 13), the moment about J due to the thrust in the deck is 30.3, and the moment in the arch rib is 20.7, giving a total of 68.6, which is greater than 43. By comparison, the figure for the arch rib alone is only 20.7, which is less than 43. The important item is evidently the thrust 11.2. It will be seen from

Table 13. Check for statical equilibrium in the case of the applied loading of 100 tons at point P

Section just left of Post No.	2	3	4	5	6
Shear Q in post on left	–0.76	–5.93	–10.26	7.55	18.60
Thrust T in deck $= \Sigma Q$	–0.76	–6.69	–16.95	–9.40	9.20
$T \cdot h$	–4.50	–26.70	–47.20	–21.00	20.90
Moment M_d in deck	7.65	–52.42	– 6.77	14.37	16.24
Moment M_r in rib	4.62	–80.07	– 5.87	14.99	14.54
$M_r + M_d + T \cdot h$	7.77	–159.19	–59.84	8.36	51.68
External moment	*–7.5*	*158.3*	*58.9*	*–9.6*	*–52.5*
% M resisted by T		17%	79%		40%
Section just right of Post No.	5	6	7	8	9
Shear Q in post on right	–8.10	6.00	7.71	3.06	0.43
Thrust T in deck $= \Sigma Q$	9.10	17.20	11.20	3.49	0.43
$T \cdot h$	–20.70	–38.80	–30.30	–14.98	–2.56
Moment M_d in deck	6.38	–7.03	–17.60	–17.88	1.05
Moment M_r in rib	5.97	–4.47	–20.69	–24.06	–6.40
$M_r + M_d + T \cdot h$	–8.35	–50.3	–68.59	–56.92	–7.90
External moment	*9.6*	*52.0*	*69.80*	*56.2*	*7.6*
% M resisted by T		77%	44%	26%	32%

Table 13 that the percentage of the moment resisted through the balancing action of this thrust is considerable, amounting to 79% for the section just to the left of post 4 and 77% for the section just to the right of post 6. Consequently, moments in the arch rib in panels where the resultant line of thrust has been moved further from the arch rib and where an increase in these moments might have been expected are, in fact, less than the corresponding moments produced by the same load in the same arch rib without a deck. This reduction is considerable and may amount to more than 60%, as will be seen by a comparison of the bending-moment diagrams for the arch rib and deck and the arch rib only (Fig. 17).

So far, the role played by the deck has been an assisting role, but it is of interest to enquire into the stresses produced in the deck itself and the extent to which the thrust in the arch rib has changed. Large moments have developed in the deck, greater even than was suggested by NEWMARK[15]) who claims a moment distribution between the arch rib and deck in the ratio of the moments of inertia of their cross sections. Furthermore, a comparatively large thrust has been transmitted to the deck through the shear in the spandrel columns.

[15]) NEWMARK, "Interaction between Rib and Superstructure in Concrete Arch Bridges", Transactions, American Society of Civil Engineers, vol. 103, 1938.

Table 14. Ratios of the thrust in the deck and the horizontal thrust in the rib to the horizontal reaction at the abutments

Panel	I	II	III	IV	V	VI	VII	VIII	IX
Thrust T in deck	−0.76	−6.69	−16.95	−9.40	9.20	17.20	11.20	3.49	0.43
Horizontal thrust H_r in rib	45.94	40.01	29.75	37.3	5.97	63.90	57.90	50.19	47.13
T/H (%)	1.65	14.4	36.3	20.2	−19.7	−36.9	−24.0	−7.5	−0.9
H_r/H (%)	98.35	85.6	63.7	79.8	119.7	136.9	124.0	107.5	100.9

As will be seen from Table 14 this thrust, which may be either tensile or compressive, reaches 37% of the horizontal reaction at the springings in panels III and VI. In panels where the deck is in compression, the arch rib is relieved of a part of the thrust which would otherwise have existed. On the other hand, where the deck is in tension, the arch rib carries a greater thrust than that due to the full external reaction alone. In panel VI, the horizontal compressive force H in the arch rib is as high as 137% of the horizontal reaction at the springing owing to a tensile force, equal to 37% of this reaction, which has developed in the deck. This is therefore a harmful contribution by the deck to the arch rib. In general, this harmful contribution is to be expected where the resultant line of thrust falls outside the open-spandrel arch panel.

Conclusions

A method has been evolved which provides an exact solution without the need for solving the considerable number of elastic equations necessary in the classical methods. All computations are reduced to a form in which they may be made by slide rule. Multiple open-spandrel arch systems may equally be solved as, by this method, the elastic constants for particular spans become readily available.

Comparison with some experimental results shows exceedingly close agreement. The shear resistance of the spandrel columns is shown to be an important item in deck participation, enabling a large thrust to be transferred to the deck.

Summary

Designers of arch bridges have long recognised the existence of interactions between the arch rib, the spandrel columns and the deck in the case of open spandrel structures having full continuity.

The theoretical analysis of such a structure has, however, always been regarded as so complicated that it has seldom been undertaken. Experimental evidence has provided some indication of the effects of deck participation in the stresses but there has been no information as to the quantitative distribution of stresses between the arch rib and the deck.

In this paper a method of theoretical analysis is developed which enables the interactions between the arch rib, the spandrel columns and the deck to be taken into account.

The elastic properties of the structure, valid for all conditions of loading, are first evaluated; once this has been done the effects of any desired loading conditions can be quite rapidly determined. In this method, elastically equivalent closed panels are used in replacement of the whole structure. The process employs only simple arithmetical operations and no simultaneous equations so that the whole solution becomes a slide rule job.

The method is applied to a case for which experimental results are available and, where comparison can be made, agreement is found to be very good. The theoretical analysis, however, yields much information that was not available from the experimental work.

The method can be used to investigate stresses due to particular loadings, influence lines for desired stress components, effects of expansion joints, temperature effects, etc., and can be applied equally to the solution of multiple arch systems.

Résumé

Les spécialistes du calcul des ponts en arc, ont depuis longtemps reconnu l'existence d'influences réciproques entre les membrures de l'arc, les colonnes du tympan et le tablier, dans le cas des ouvrages à tympan ouvert présentant une pleine continuité.

L'étude théorique d'un tel ouvrage a toutefois été toujours considérée comme si complexe qu'elle n'a été qu'assez rarement entreprise. La pratique expérimentale a fourni quelques indications sur l'influence de la participation du tablier aux contraintes; toutefois, nous ne disposons d'aucune information sur la répartition quantitative des contraintes entre les membrures de l'arc et le tablier.

L'auteur du présent rapport expose une méthode d'analyse théorique qui permet de tenir compte des actions réciproques entre la membrure de l'arc, les colonnes du tympan et le tablier.

Il détermine tout d'abord les propriétés élastiques de l'ouvrage, propriétés valables pour toutes les conditions de charge; après cette première étude, il est possible de déterminer très rapidement l'influence de toutes les conditions de charges voulues. Dans cette méthode, l'ensemble de l'ouvrage est remplacé

par des panneaux fermés élastiquement équivalents. Ce procédé ne fait intervenir que des opérations arithmétiques simples, sans systèmes d'équations, de sorte que dans son ensemble la solution ne constitute qu'un travail de règle à calcul.

Cette méthode est appliquée à un cas pour lequel nous disposons déjà de résultats expérimentaux et où les comparaisons révèlent une excellente concordance. Toutefois, l'étude théorique fournit de nombreuses informations qu'il était impossible de tirer de l'étude expérimentale.

Cette méthode peut être utilisée pour les recherches importantes sur les points suivants: contraintes dues à des charges particulières, lignes d'influence relatives à des composantes déterminées, influence des joints de dilatation, influence de la température, etc. La méthode peut également être appliquée à la solution des systèmes à arcs multiples.

Zusammenfassung

Bei der Konstruktion von Bogenbrücken wurde das Vorhandensein von Wechselwirkungen zwischen den Bogenrippen, den Stützen und der Fahrbahn bei Tragwerken mit monolithischem Zusammenhang schon lange erkannt.

Die theoretische Berechnung solcher Tragwerke wurde jedoch immer als so kompliziert angesehen, daß sie selten durchgeführt wurde. Versuche lieferten die Anzeichen für das Mitwirken der Fahrbahn, aber sie gaben keinen Aufschluß über die quantitative Verteilung der Spannungen auf Bogenrippen und Fahrbahn.

Im vorliegenden Beitrag wird eine Berechnungsmethode entwickelt, welche die Berücksichtigung des Zusammenwirkens von Bogen, Stützen und Fahrbahn ermöglicht.

Die elastischen Eigenschaften, die für alle Belastungsfälle gültig sind, werden zuerst berechnet; wenn das geschehen ist, kann die Wirkung jedes einzelnen Belastungsfalls ziemlich rasch bestimmt werden. Die Konstruktion wird für die Berechnung ersetzt durch elastisch äquivalente geschlossene Rahmenfelder. Der Rechnungsgang erfordert nur einfache arithmetische Operationen und keine Auflösung von Gleichungssystemen, so daß die ganze Berechnung mit dem Rechenschieber durchgeführt werden kann.

Die Methode wird auf einen Fall angewendet, bei dem Versuchsresultate verfügbar sind. Die Vergleiche zeigen eine gute Übereinstimmung der Resultate. Die theoretische Berechnung liefert jedoch viele Aufschlüsse, die aus den Versuchen nicht erhältlich waren.

Die Methode kann verwendet werden zur Untersuchung von Spannungen infolge Teilbelastung, von Einflußlinien für bestimmte Spannungskomponenten, der Wirkung von Dilatationsfugen, von Temperaturwirkungen, usw. Sie kann auch zur Berechnung von Bogenteilen herangezogen werden.